Journal of Hip Preservation Surgery, 2025, **11**, 243–250
DOI: https://doi.org/10.1093/jhps/hnae020
Advance access publication date: 25 June 2024
Research article

Understanding recurrent groin pain following periacetabular osteotomy: assessment of psoas tendon mechanics using discrete element analysis

Karadi H. Sunil Kumar[1*], Floris Van Damme[2], Ide Van den Borr[2], Vikas Khanduja[3], Emmanuel Audenaert[2] and Ajay Malviya[1,4]

[1]Wansbeck General Hospital, Northumbria Healthcare NHS Foundation Trust, Ashington, UK, [2]UZ Gent, University of Ghent, C. Heymanslaan 10, Ghent 9000, Belgium, [3]Addenbrookes—Cambridge University Hospitals NHS Trust, Hills Road, Cambridge CB2 0QQ, UK and [4]Newcastle University, Newcastle upon Tyne NE1 7RU UK.

[*]**Correspondence to**: K. H. Sunil Kumar. **E-mail**: drkhskumar@yahoo.com

ABSTRACT

Recurrent groin pain following periacetabular osteotomy (PAO) is a challenging problem. The purpose of our study was to evaluate the position and dynamics of the psoas tendon as a potential cause for recurrent groin pain following PAO. A total of 386 PAO procedures, performed between January 2013 and January 2020, were identified from a single surgeon series. Thirteen patients (18 hips) had a psoas tendinopathy, as confirmed with relief of symptoms following a diagnostic injection into the psoas tendon. All patients underwent computed tomography (CT) scans pre- and post-operatively. The data from CT scan was used to manually segment bony structures and create 3D models using Mimics software (Materialise NV). A validated discrete element analysis model using rigid body springs was used to predict psoas tendon movement during hip circumduction and walking. The distance of the iliopsoas tendon to any bony abnormality was calculated. All computational analyses were performed using MATLAB software. Thirteen hips (13/18) showed bony malformations (spurs, hypertrophic callus or delayed union and malunion) secondary to callus at the superior pubic ramus. The mean minimal distance of the iliopsoas tendon to osteotomy site was found to be 13.73 mm ($\sigma = 3.09$) for spurs, 10.99 mm ($\sigma = 2.85$) for hypertrophic callus and 11.91 mm ($\sigma = 2.55$) for canyon type. In normal bony healing, the mean minimal distance was 18.55 mm ($\sigma = 4.11$). Using a validated computational modelling technique, this study has demonstrated three different types of malformation around the superior pubic osteotomy site, which are associated with psoas impingement. In all of the cases, the minimal distance of the iliopsoas tendon to the osteotomy site was reduced by 59–74%, as compared with the normal anatomy.

INTRODUCTION

Hip dysplasia (HD) is a condition characterized by insufficient acetabular coverage of the femoral head [1, 2]. The stability of the hip joint is improved by both the anterior hip capsule and iliopsoas tendon acting as anterior stabilizers with the contribution of gluteus medius and minimus muscles acting as lateral stabilizers [3–6]. Patients with HD often present with pain related to muscles and tendons around the hip [7–10]. Pre-operatively nearly one in five cases of HD reported pain attributed to the iliopsoas tendon which was attributed as the cause of low functional outcomes in these patients [11]. In addition, a frequently diagnosed condition in dysplastic hips is the internal snapping hip syndrome related to the iliopsoas tendon, with some studies reporting a prevalence of up to 30% [5, 6, 12]. Furthermore, patients with HD have altered gait patterns, resulting in altered muscle torques while performing abduction and external rotation of the hip. They also have an increased gluteus medius muscle volume with significantly shorter muscle moment arms along with a slightly lower average isometric torque, in symptomatic HD patients when compared to controls, for the hip abductors, extensors and flexors [10]. As a result, patients may experience pain in these muscles relating to overuse [5]. The iliopsoas muscle is an important muscle during walking, running and standing upright [6, 13–16]. Iliopsoas is the main flexor of the hip and is made up of three different muscles: the psoas major, the psoas minor and the iliacus muscle. The tendon of the iliopsoas muscle usually consists of both the iliacus and the psoas major muscle, but variations may occur. The psoas minor muscle is inconsistent and may be absent in up to 40% of the population [3, 13–15, 17].

Received 7 February 2023; revised version accepted 6 June 2024

Periacetabular osteotomy (PAO) has gained importance as a joint-preserving procedure for the treatment of symptomatic acetabular dysplasia [2, 18, 19]. PAO is a re-directional osteotomy (Fig. 1) of the acetabulum which preserves the integrity of the hip joint and improves function [19, 20]. It involves osteotomy of the superior pubic ramus, the iliac wing and up to 50% of the width of the posterior column and ischium. The ischial osteotomy is a partial osteotomy to ensure that the osteotomy leaves an acceptable amount of intact posterior column allowing early assisted weight bearing. The superior pubic ramus osteotomy is performed just medially to the iliopectineal eminence, which is near the path of the iliopsoas tendon raising the possibility of interference of the tendon after surgery [21, 22]. In particular, concerns have been raised about the position of the superior pubic ramus osteotomy. If performed more medially, the osteotomy would likely interfere with the femoral vessels passing through the vascular lacuna [3, 21, 22]. If performed more laterally, the broader bony surface may predispose to excessive callus formation and the formation of spurs, or pseudarthrosis. This may in turn lead to irritation of the iliopsoas tendon with consequent groin pain [3, 12, 23]. Recurrent groin pain following PAO is a difficult problem and determining the aetiology of pain in these patients can be very challenging, even for the experienced surgeon.

The aim of this study was to evaluate the position and dynamics of the psoas tendon as a potential cause for recurrent groin pain following PAO due to its proximity to the osteotomy site of the superior pubic ramus [5, 6].

MATERIALS AND METHODS

Patients with recurrent ipsilateral hip pain following PAO were identified from a comprehensive prospectively collected PAO database at an academic referral centre between January 2013 and January 2020. A total of 386 PAOs were performed during the study period by a single experienced surgeon (A.M.). Patients presenting with recurrent or residual groin pain were further assessed with plain radiograph, ultrasound scan (USS), CT scan and MRI scans, as deemed necessary to look for degeneration, stress fractures, delayed non-union and soft-tissue causes. Patients who presented with signs and symptoms suggestive of psoas tendinopathy that did not resolve with physiotherapy underwent a hip USS-guided iliopsoas injection to confirm the diagnosis. The patients where the tendinopathy did not resolve were those who underwent a further CT scan to assess the 3D morphology of the hip and the osteotomy site. A total of 18 hips in 13 patients, who responded positively to the USS-guided iliopsoas injection but had ongoing symptoms, were included in the study. Bone geometry of both the pelvis and the knees was derived from this data by manual segmentation using a dedicated 3D software program Mimics (Materialise NV, Leuven, Belgium). The data set involved high-resolution CT images with an inter-voxel spacing ranging from 0.578 to 0.977 mm and an inter-slice thickness of either 0.625 or 1.250 mm. Different bony structures were separated using the split mask tool and minor reconstruction errors were manually corrected using the edit mask tool and then exported separately as .STL file which could then be used to perform simulations of psoas tendon excursion using a previously established discrete element analysis (DEA) model [24]. The femoral bony anatomy, in particular the missing intercalating femoral diaphysis, was completed by fitting a detailed shape model of the femur [25].

All patients underwent assessment of radiographical parameters (Fig.2) such as femoral neck-shaft angle, femoral offset, femoral anteversion, anterior centre edge angle (ACEA) and acetabular version from CT images using an integrated tool in Mimics software. Simulated plain radiographs were created from the CT data using Mimics to assess the lateral centre edge angle (LCEA), Tönnis angle and acetabular index (AI). All measurements were performed by one author who had been appropriately trained (F.V.D.) using previously published techniques. In addition, LCEA and AI were measured separately from the preoperative plain radiograph of the pelvis by the senior author (A.M.). Detailed description of these radiographical parameters is provided in Fig. 2 and the measurements are shown in Table I.

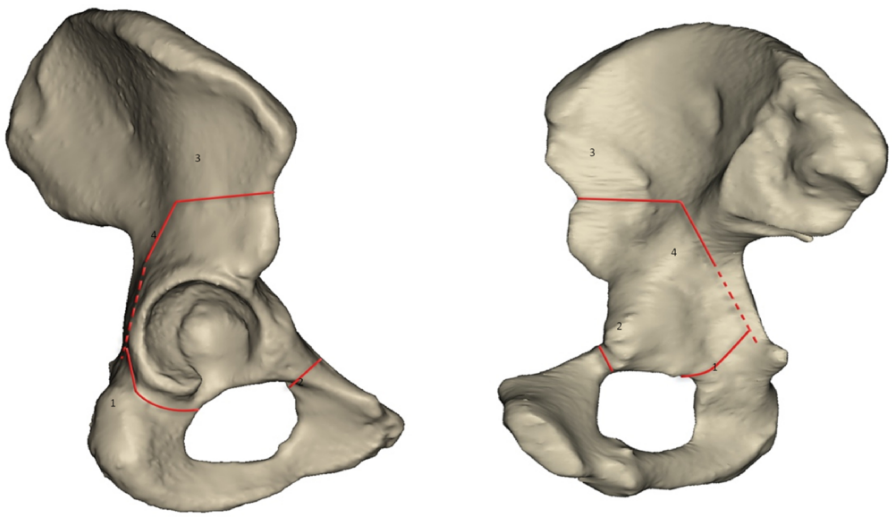

Fig. 1. Schematic representation of the osteotomy cuts performed in Bernese.

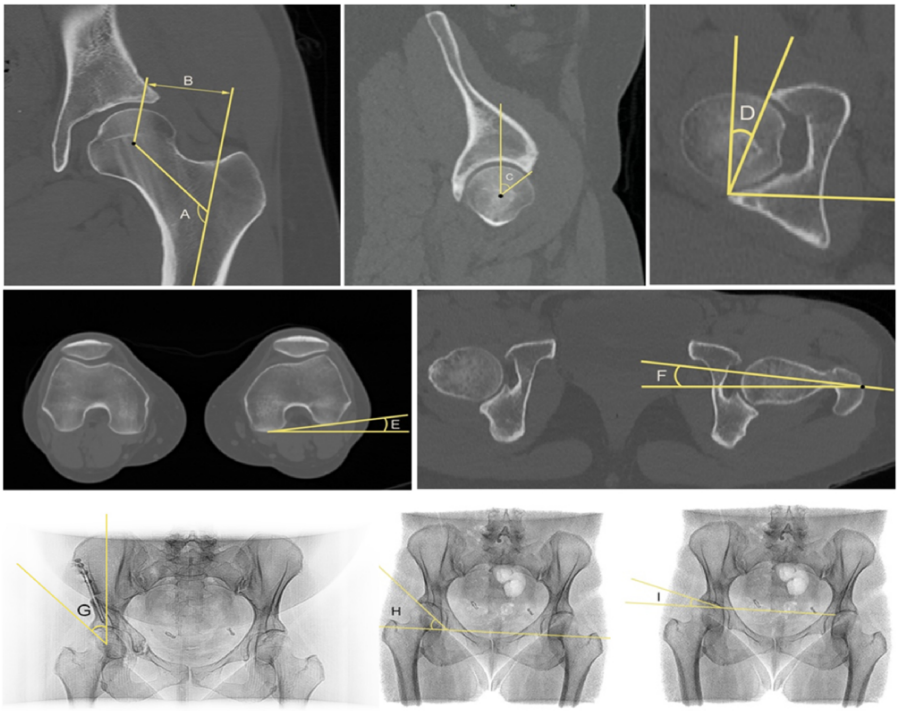

Fig. 2. Radiographic measurements on CT (**A**–**F**) and generated x-ray (**G**–**I**).

Table I. Radiographic parameters describing variation in hip joint morphology

			Mean (σ)	
Parameter	***Definition***	***Reference values***	***Preoperative (N = 18)***	***Postoperative (N = 18)***
Femoral neck-shaft angle (A)	Angle formed by the axis of the femoral neck and the proximal femoral diaphyseal axis on antero-posterior view, indicating varus or valgus formation of the femur	125–135°	130.84 (3.96)	—
Femoral offset (B)	The distance from the centre of rotation of the femoral head to a line bisecting the long axis of the femur	25–60 mm	33.07 (4.29)	—
ACEA (C)	Amount of femoral head coverage by the anterior aspect of the acetabular roof	34–66°	47.76 (6.96)	52.30 (4.11)
Acetabular anteversion (D)	Angle formed by the sagittal plane and a line connecting anterior/posterior acetabular edge midfemoral, indicating acetabular orientation	11–23°	21.61 (4.06)	39.49 (5.74)
Femoral anteversion (E + F)	Angle formed by the axis of the femoral neck and the femoral shaft, indicating the degree of femoral torsion	8–15°	18.13 (8.55)	
LCEA (G)	Amount of femoral head coverage by the most cranial aspect of the acetabular roof (sourcil)	25–39°	17.00 (3.95)	35.97 (3.12)
Acetabular angle by sharp (H)	Angle formed by a horizontal line through the inferior of the teardrop and a line from this point to the lateral acetabular margin, used to evaluate hip dysplasia	33–38°	41.9 (3.2)	28.4 (3.8)
Tönnis angle/AI (I)	Amount of bony acetabular coverage of the femoral head, indicated by the angle formed by a line extending from the medial to the lateral edge of the sourcil and the horizontal plane	5–15°	12.97 (4.31)	–0.64 (4,57)

A validated DEA model using rigid body springs was used to predict psoas tendon movement during hip circumduction and walking [24, 26, 27]. For each motion step, the elastic-constrained path of the tendon and muscle was calculated. The model was used to compare the preoperative and postoperative psoas tendon trajectory in sagittal, coronal and axial planes. Additionally, the distance of the psoas tendon in relation to the superior pubic ramus osteotomy site was noted by measuring the minimal distance between the tendon and osteotomy. The minimum distance for the tendon varied only minimal during gait per patient and no significant pattern could be identified. The hip joint was modelled as a spherical joint with three rotational degrees of freedom [28]. Considering gait only requires a minimal of 20–30° of angular hip flexion, the tendon's position was mainly dictated by the skeletal anatomy rather than variance in kinematics. However, during simulation of circumduction, the minimal distances were observed at minimal adduction positions [28]. Gender-specific hip rotations during walking were obtained from the documented cases of the Orthoload Database (https://orthoload.com/) and subsequently imposed on the 3D surface models [27, 29]. In patients with radiographical evidence of bony spur formation near the predicted path of the psoas tendon, the minimal distance between the tendon and the spur was calculated using the same *k*-nearest neighbour search. All computational analysis was performed using MATLAB software. Psoas tendon simulations are shown in Fig. 3.

RESULTS

A total of 386 PAO procedures were performed in our centre between January 2013 and January 2020 with a minimum 2-year post-operative follow-up. Thirteen patients with 18 hips (4.7%) with confirmed psoas tendinopathy, based on the response to local injection and exclusion of other contributory pathology, underwent additional CT imaging. All subjects included were female with an average age of 41.2 years.

The DEA model did not find any significant alteration in simulated psoas tendon movements during hip circumduction and walking in sagittal, coronal and axial planes when comparing the preoperative CT scan with the dynamics of the tendon after PAO.

All 3D surface models of the affected hips were inspected digitally to determine possible bony malformations at the osteotomy site in those who presented with recurrent hip pain postoperatively. Five models showed no sign of malformation around the osteotomy sites and were considered to have healed properly. The remaining 13 postoperative models (72%) showed signs of moderate to severe malformation, primarily of the superior pubic osteotomy. These malformations were broadly categorized into three patterns: (I) bony spur, (II) hypertrophic callus or delayed union and (III) canyon-type malalignment. The most common of these malformations was the formation of spurs close to the osteotomy site which were near the expected path of the psoas tendon. The second type of malformation was a hypertrophic callus or delayed union type, where the two osteotomized bony fragments did not fully unite resulting in a broader and uneven superior pubic ramus near the predicted path of the psoas tendon. Finally, the third category was defined as a canyon-type malalignment, where the bony fragments united but did not remodel to form a smooth bony surface. Instead, there was 'step' in the superior pubic ramus following healing which most likely interfered with normal psoas tendon excursion. These three different categories are illustrated in Figs 4 and 5. Of the 13 hips with evidence of bony malformation, 4 (31%) were identified as primarily spur-type, 6 (46%) were primarily hypertrophic callus or delayed union-type and 3 (23%) were canyon-type malformations. In two cases of hypertrophic callus, there was also evidence of visible spur-formation.

The mean minimal distance of the psoas tendon to the osteotomy site of the superior pubic ramus during circumduction and gender-specific walking motion of the hip is shown in Table II. The mean minimal distance of the iliopsoas tendon to the osteotomy site was found to be 13.73 mm ($\sigma = 3.09$) for spur type, 10.99 mm ($\sigma = 2.85$) for hypertrophic callus/delayed union type and 11.91 mm ($\sigma = 2.55$) for canyon type. In cases with normal bony healing ($n = 5$), a considerably larger mean minimal distance of 18.55 ($\sigma = 4.11$) was noted. In cases with

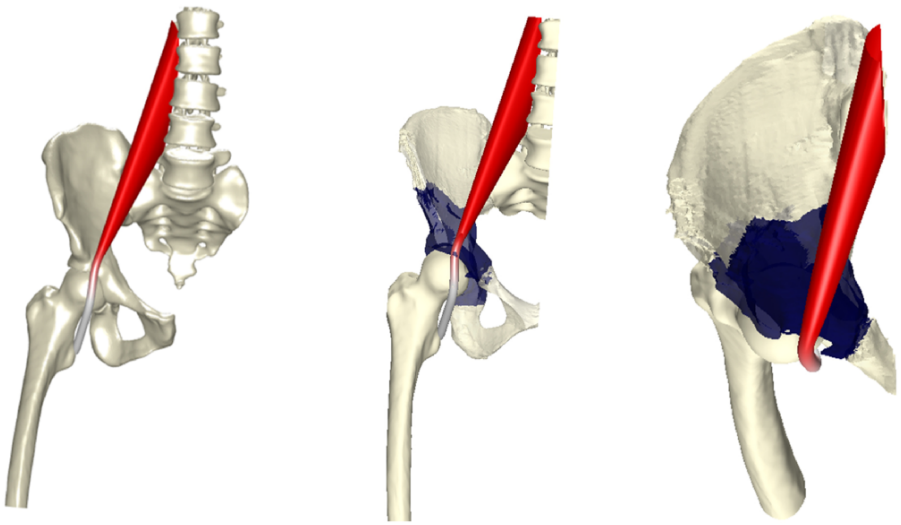

Fig. 3. Psoas tendon simulation post osteotomy during walking and hip circumduction.

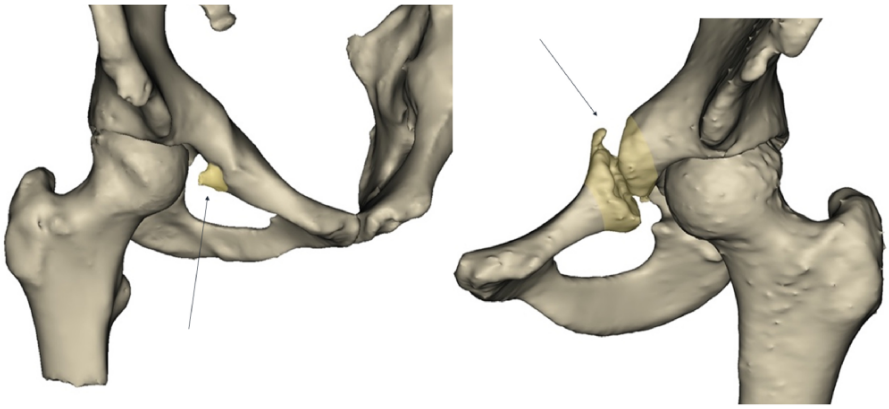

Fig. 4. Osteophyte formation (left) and hypertrophic callus/delayed union (right).

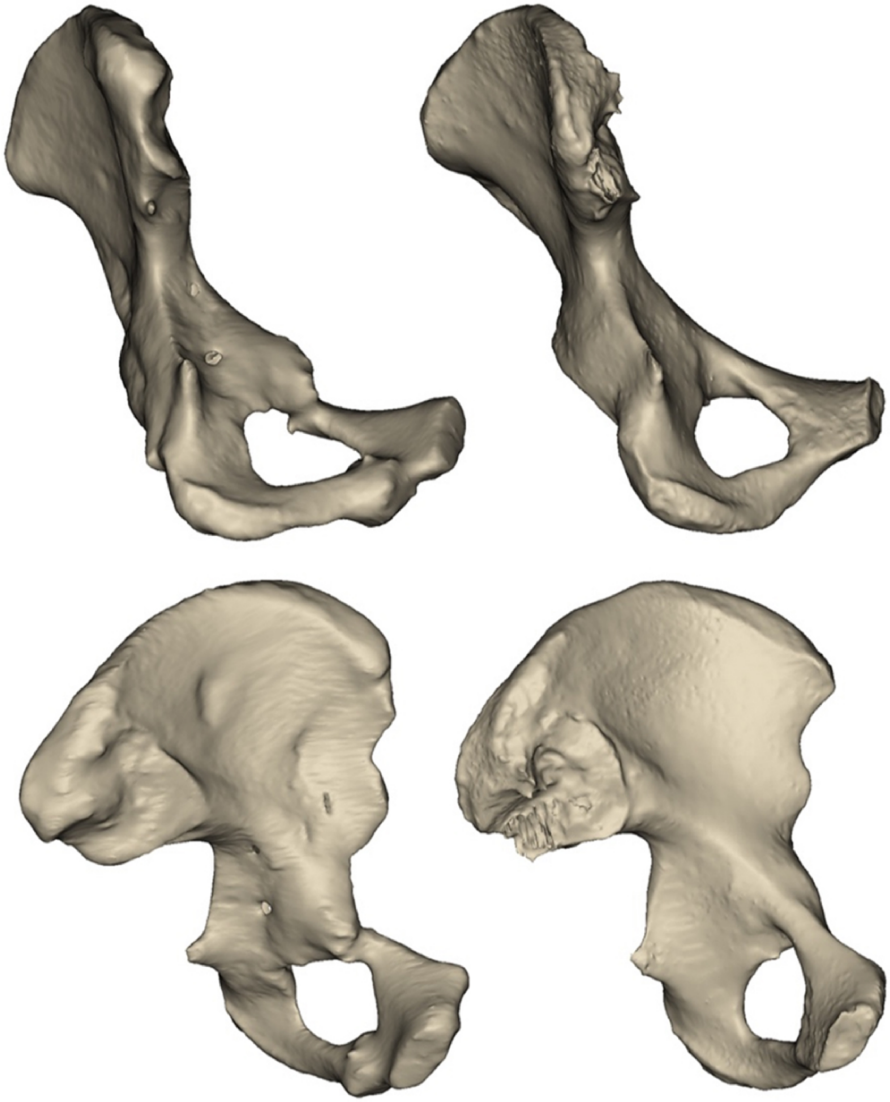

Fig. 5. Canyon-type malunion (left) compared to normal upper pubic arch (right).

Table II. Minimal distance of iliopsoas tendon to osteotomy site (mm)

Spur type Mean (σ) N = 4	*Hypertrophic callus/delayed union type Mean (σ) N = 6*	*Canyon type Mean (σ) N = 3*	*Normal bony healing Mean (σ) N = 5*
13.73 (3.09)	10.99 (2.85)	11.91 (2.55)	18.55 (4.11)

radiographical evidence of spur-formation ($n = 6$, pure spur type = 4, combined spur and hypertrophic callus = 2), the mean minimal distance of the psoas tendon to these spurs was found to be 6.24 mm ($\sigma = 1.88$). The minimal distance of the iliopsoas tendon to the osteotomy site in individual cases is shown in Table III.

DISCUSSION

Our study is the first to report the anatomical relationship between the iliopsoas tendon and the superior pubic ramus osteotomy site to improve our understanding of the causes of recurrent or persistent groin pain following PAO surgery. PAO is a successful joint-preserving procedure in symptomatic HD with several authors reporting good long-term outcomes [12, 18, 30–32]. Although failure rates in terms of early conversion to joint arthroplasty are low, patients do complain of pain and discomfort which persist even following metalwork removal [33, 34]. Some causes of these symptoms include delayed or non-union, progressive damage to articular cartilage and irritation of surrounding soft tissues, most commonly the iliopsoas muscle and tendon [35]. Even though several studies report good long-term outcome data following PAO, there is a paucity of literature reporting on iliopsoas issues post-PAO [12, 33]. We have tried to answer this question by objectively assessing the morphology of the pelvis using 3D reconstructions and simulate the psoas dynamics to understand this problem. We have found that simulated psoas tendon movement during hip circumduction and walking do not alter after PAO in any plane as compared with preoperative dynamics.

Evaluating the bony morphology showed three distinct types of malformations at the superior pubic osteotomy site. The proximity of the iliopsoas muscle and tendon to the superior pubic osteotomy is of considerable importance. The iliopsoas muscle is retroperitoneal and crosses the pelvi brim over the superior pubic ramus before inserting into the lesser trochanter. The muscle becomes a tendon after crossing the superior pubic ramus [36]. The iliopsoas tendon is formed mainly of the psoas major with some contribution from the iliacus [36]. The iliopsoas tendon is commonly involved in cases of HD due to irritation from the shallow acetabulum and in some cases concomitant increased femoral anteversion [6]. The iliopsoas tendon has an important role in stabilizing the femoral head in HD cases. We identified three distinct types of bony malformations: spur, hypertrophic callus or delayed union and canyon type. Specifically, the bony protrusions seen in spur-formation and hypertrophic callus could potentially affect the smooth excursion of the iliopsoas tendon. In certain postoperative cases, resulting iliopsoas tendinitis could explain the recurring groin pain incurred by these patients [5, 6].

In our series, 13 out of the 18 hips showed evidence of bony malformation. The majority of these were spurs and hypertrophic callus. In five hips, the osteotomy had healed normally without any evidence of bony malformation. We found that the distance between the iliopsoas tendon and the osteotomy site was significantly less (59–74% lesser) in those cases with bony malformations (spur type = 13.73 mm, hypertrophic callus = 10.99 mm versus normal = 18.55 mm) when compared to those with normal bony healing. The reduced distance may be secondary to a tight psoas tendon causing irritation around the osteotomy site and further pain. Furthermore, when evaluating the distance between the iliopsoas tendon and the spurs, we found that the mean minimal distance was further reduced to 6.24 mm ($\sigma = 1.88$). This raises the possibility that potentially the resultant spurs had a role in iliopsoas tendon irritation. However, our computational analysis predicted that in none of the cases the iliopsoas tendon came into direct contact with the bony malformations. Interestingly, the distance of the iliopsoas tendon to the malformations was considerably higher in cases with normal bone healing, which raises the question whether the iliopsoas tendon played a role in interfering with the bone healing or if the altered bone healing leads to iliopsoas issues. If the latter is true, then that can only be possible if the bony malformations indirectly interfered with psoas tendon movement by affecting surrounding soft tissues. Some authors have hypothesized that the iliopsoas tendon near the superior pubic osteotomy might interfere with normal healing following PAO predisposing to bony malformations [21, 22]. Furthermore, the interfragmentary strain between the two fragments varies depending on whether the patient is full or partial weight bearing in the immediate post-operative period and also depends on the forces going through each fragment [37]. This would infer that the closer the muscle is to the fragment the force would possibly be higher. We could not find any article specifically mentioning about the muscle forces at the osteotomy site and healing. Hopefully, the current pilot study will form the basis of further research to enhance understanding in this field.

LIMITATIONS

This study has several limitations that need to be discussed. The first is a limited sample size of 13 patients totalling 18 osteotomies with unresolved psoas tendinopathy. Making assumptions based on this relatively sparse data set is therefore difficult. This is further accentuated by the fact that all included subjects were female. Interestingly we did not note any male patient with persistent psoas tendinopathy after PAO in our series. Secondly, we have not been able to compare the CT scan findings with a cohort of asymptomatic patients as we do not routinely perform a post-operative CT scan unless indicated to avoid unnecessary radiation exposure. Thirdly, these cases spanned a period of around 8 years including the learning curve of the senior author (A.M.) who performed all cases of PAO. It is possible that during this time, modifications to the operating

Table III. Individual measurements of minimal distance of iliopsoas tendon to spurs and osteotomy site (mm) (NA - not applicable)

Case	*PAO side*	*Comments*	*Distance to spur*	*Distance to osteotomy*
1	R	Spur	4.63	18.07
	L	Non-operated hip	NA	NA
2	R	Spur	4.94	14.58
	L	Canyon type	NA	8.31
3	R	Hypertrophic callus/non-union	4.87	10.23
	L	Non-operated hip	NA	NA
4	R	Normal healing	NA	23.29
	L	Non-operated hip	NA	NA
5	R	Hypertrophic callus/non-union	NA	14.25
	L	Spur	9.92	12.71
6	R	Normal healing	NA	20.09
	L	Canyon type	NA	13.74
7	R	Non-operated hip	NA	NA
	L	Normal healing	NA	11.44
8	R	Normal healing	NA	16.86
	L	Non-operated hip	NA	NA
9	R	Non-operated hip	NA	NA
	L	Normal healing	NA	21.06
10	R	Non-operated hip	NA	NA
	L	Hypertrophic callus/non-union	NA	11.86
11	R	Hypertrophic callus/non-union	NA	7.75
	L	Non-operated hip	NA	NA
12	R	Hypertrophic callus/non-union	7.31	7.31
	L	Hypertrophic callus/non-union	NA	14.54
13	R	Spur	5.74	9.54
	L	Canyon type	NA	13.68

technique were made to lower the risk for potential postoperative soft tissue complications.

Recurrent hip pain following PAO is a challenging problem even for an experienced surgeon [11]. Some authors have performed diagnostic hip arthroscopy to determine a possible intra-articular cause with high numbers of intra-articular lesions identified in these patients [11, 35]. However, establishing a definitive link between the intra-articular pathology and the groin pain has been difficult. Selective intra-articular hip injections may help differentiate intra-articular causes of pain from extra-articular causes and guide treatment strategies [12].

CONCLUSION

Recurrent groin pain following PAO is a difficult problem. Evaluating the iliopsoas tendon as a cause of postoperative pain may prove difficult. The use of CT scan can help identify any bony malformations which could potentially be the cause of this problem. Dynamic ultrasound visualization of the psoas tendon might provide valuable information in addition to clinical assessment and allow for targeted injection to this area. In this study, using computational modelling techniques, we have demonstrated that the psoas tendon trajectory is altered in patients with psoas-related pain after a PAO. The mean distance between the iliopsoas tendon and the osteotomy site was significantly lower in patients with psoas-related pain when compared to those patients who underwent good bone re-modelling of the osteotomy site. We have proposed three different types of malformations at the superior pubic osteotomy site which have a potential to impeding normal tendon function following PAO. Further large-scale prospective studies are warranted to further investigate the soft tissue complications following PAO surgery, as well as to provide effective treatment strategies.

DATA AVAILABILITY

The data underlying this article will be shared on reasonable request to the corresponding author.

ACKNOWLEDGEMENTS

None.

CONFLICT OF INTEREST STATEMENT

V.K. is a consultant at Smith and Nephew, Stryker, and Arthrex; an Associate Editor-in-Chief at *JISAKOS*; on the Editorial Boards of IO, *Open Access Journal of Sports Medicine, IJO*, and *JTO*; and a board member of SICOT, ISAKOS, ISHA, NAHR, and BOA. A.M. is a past chair of NAHR; a consultant at Pfizer, Smith & Nephew, and NTL Biologica; and an associate editor of *JHPS*. All other authors have no conflicts of interest to declare.

FUNDING

No funding was received for this study.

REFERENCES

1. Wilkin GP, Ibrahim MM, Smit KM *et al*. A contemporary definition of hip dysplasia and structural instability: toward a comprehensive classification for acetabular dysplasia. *J Arthroplasty* 2017; **32**: S20–7.

2. Pascual-Garrido C, Harris MD, Clohisy JC. Innovations in joint preservation procedures for the dysplastic hip 'the periacetabular osteotomy'. *J Arthroplasty* 2017; **32**: S32–7.
3. Dimon JH. Surgical anatomy of the hip. *Surg Clin North Am* 1974; **54**: 1327–35.
4. Rydell N. Biomechanics of the hip-joint. *Clin Orthop Relat Res* 1973; **92**: 6–15.
5. Jacobsen JS, Hölmich P, Thorborg K *et al.* Muscle-tendon-related pain in 100 patients with hip dysplasia: prevalence and associations with self-reported hip disability and muscle strength. *J Hip Preserv Surg* 2017; **5**: 39–46.
6. Jacobsen JS, Bolvig L, Hölmich P *et al.* Muscle-tendon-related abnormalities detected by ultrasonography are common in symptomatic hip dysplasia. *Arch Orthop Trauma Surg* 2018; **138**: 1059–67.
7. Garbuz DS, Masri BA, Haddad F *et al.* Clinical and radiographic assessment of the young adult with symptomatic hip dysplasia. *Clin Orthop Relat Res* 2004; **418**: 18–22.
8. Nunley RM, Prather H, Hunt D *et al.* Clinical presentation of symptomatic acetabular dysplasia in skeletally mature patients. *J Bone Joint Surg Am* 2011; **93**: 17–21.
9. Gala L, Clohisy JC, Beaulé PE. Hip dysplasia in the young adult. *J Bone Joint Surg Am* 2016; **98**: 63–73.
10. Harris MD, Shepherd MC, Song K *et al.* The biomechanical disadvantage of dysplastic hips. *J Orthop Res* 2022; **40**: 1387–96.
11. Jacobsen JS, Søballe K, Thorborg K *et al.* Patient-reported outcome and muscle-tendon pain after periacetabular osteotomy are related: 1-year follow-up in 82 patients with hip dysplasia. *Acta Orthop* 2019; **90**: 40–5.
12. Larsen JB, Mechlenburg I, Jakobsen SS *et al.* 14-year hip survivorship after periacetabular osteotomy: a follow-up study on 1,385 hips. *Acta Orthop* 2020; **91**: 299–305.
13. Regev GJ, Kim CW, Tomiya A *et al.* Psoas muscle architectural design, in vivo sarcomere length range, and passive tensile properties support its role as a lumbar spine stabilizer. *Spine (Phila Pa 1976)* 2011; **36**: E1666–74.
14. Philippon MJ, Devitt BM, Campbell KJ *et al.* Anatomic variance of the iliopsoas tendon. *Am J Sports Med* 2014; **42**: 807–11.
15. Neumann DA, Garceau LR. A proposed novel function of the psoas minor revealed through cadaver dissection. *Clin Anat* 2015; **28**: 243–52.
16. Yen YM, Lewis CL, Kim YJ. Understanding and treating the snapping hip. *Sports Med Arthrosc Rev* 2015; **23**: 194–9.
17. Chang CY, Huang AJ. MR imaging of normal hip anatomy. *Magn Reson Imaging Clin N Am* 2013; **21**: 1–19.
18. Clohisy JC, Schutz AL, John St L *et al.* Periacetabular osteotomy: a systematic literature review. *Clin Orthop Relat Res* 2009; **467**: 2041–52.
19. Kamath AF. Bernese periacetabular osteotomy for hip dysplasia: surgical technique and indications. *World J Orthop* 2016; **7**: 280–6.
20. Chen M, Shang XF. Surgical treatment for young adult hip dysplasia: joint-preserving options. *Int Orthop* 2016; **40**: 891–900.
21. Thawrani D, Sucato DJ, Podeszwa DA *et al.* Complications associated with the Bernese periacetabular osteotomy for hip dysplasia in adolescents. *J Bone Joint Surg Am* 2010; **92**: 1707–14.
22. Zaltz I, Baca G, Kim YJ *et al.* Complications associated with the periacetabular osteotomy: a prospective multicenter study. *J Bone Joint Surg Am* 2014; **96**: 1967–74.
23. Biedermann R, Donnan L, Gabriel A *et al.* Complications and patient satisfaction after periacetabular pelvic osteotomy. *Int Orthop* 2008; **32**: 611–7.
24. Audenaert EA, Khanduja V, Bauwens C *et al.* A discrete element model to predict anatomy of the psoas muscle and path of the tendon: design implications for total hip arthroplasty. *Clin Biomech (Bristol, Avon)* 2019; **70**: 186–91.
25. Audenaert EA, Houcke van J, Almeida DF *et al.* Cascaded statistical shape model based segmentation of the full lower limb in CT. *Comput Methods Biomech Biomed Engin* 2019; **22**: 644–57.
26. Audenaert EA, Khanduja V, Claes P *et al.* Mechanics of psoas tendon snapping. A virtual population study. *Front Bioeng Biotechnol* 2020; **8**: Article 264.
27. Audenaert EA, Duquesne K, Roeck de J *et al.* Ischiofemoral impingement: the evolutionary cost of pelvic obstetric adaptation. *J Hip Preserv Surg* 2021; **7**: 677–87.
28. Duquesne K, Galibarov P, Salazar-torres de JJ *et al.* Statistical kinematic modelling: concepts and model validity. *Comput Methods Biomech Biomed Engin* 2022; **25**: 1028–39.
29. Bergmann G, Deuretzbacher G, Heller M *et al.* Hip contact forces and gait patterns from routine activities. *J Biomech* 2001; **34**: 859–71.
30. Clohisy JC, Barrett SE, Gordon JE *et al.* Periacetabular osteotomy for the treatment of severe acetabular dysplasia. *J Bone Joint Surg Am* 2005; **87**: 254–9.
31. Lerch TD, Steppacher SD, Liechti EF *et al.* One-third of hips after periacetabular osteotomy survive 30 years with good clinical results, no progression of arthritis, or conversion to THA. *Clin Orthop Relat Res* 2017; **475**: 1154–68.
32. Steppacher SD, Tannast M, Ganz R *et al.* Mean 20-year followup of Bernese periacetabular osteotomy. *Clin Orthop Relat Res* 2008; **466**: 1633–44.
33. Edelstein AI, Duncan ST, Akers S *et al.* Complications associated with combined surgical hip dislocation and periacetabular osteotomy for complex hip deformities. *J Hip Preserv Surg* 2019; **6**: 117–23.
34. Selberg CM, Davila-Parrilla AD, Williams KA *et al.* What proportion of patients undergoing Bernese periacetabular osteotomy experience nonunion, and what factors are associated with nonunion? *Clin Orthop Relat Res* 2020; **478**: 1648–56.
35. Clohisy JC, Ackerman J, Baca G *et al.* Patient-reported outcomes of periacetabular osteotomy from the prospective ANCHOR cohort study. *J Bone Joint Surg Am* 2017; **99**: 33–41.
36. Bordoni B, Varacallo M. *Anatomy, Bony Pelvis and Lower Limb, Iliopsoas Muscle*. StatPearls, 2023. https://www.ncbi.nlm.nih.gov/books/NBK531508/.
37. Miramini S, Ganadhiepan G, Lin YC *et al.* Influence of muscle loading on early-stage bone fracture healing. *J Mech Behav Biomed Mater* 2023; **138**: 105621.